

Emanuel Almeida
EFACEC Power Transformers
emanuel.almeida@efacec.com

Pedro Pedro
EFACEC Power Transformers
pedropedro@efacec.com

Paulo Martins
Instituto Superior Técnico
pmartins@tecnico.ulisboa.pt

Carlos Silva
Instituto Superior Técnico
carlos.alves.silva@tecnico.ulisboa.pt

EVALUATION OF DIFFERENT TYPES OF STEEL UNDER HIGH LOADING RATES FOR SHORT CIRCUIT APPLICATIONS

SUMMARY

This paper draws from independent experimental results pertaining to the properties of steel loaded at high strain rates, similar to those found in power transformer short-circuits. The types of steel that were tested are common non-alloy structural steel and high strength structural steel. The experiments showed that the most common types of structural steel, when loaded at high rates, are capable of absorbing considerably more energy than in quasi-static conditions. On the other hand, the high strength structural types of steel that were tested showed no improvement in their energy absorbing characteristics at high strain rates. The paper provides some examples to show how the experimental results may be incorporated in the design of steel components for short circuit safety. The last part is focused on the plastic deformation of steel and assesses its influence on the impedance variation of the power transformer following a short circuit.

Key words: Shell form transformers, short-circuit, dynamic analysis, material high loading rate

1. INTRODUCTION

Transformers are electrical machines placed in networks that may occasionally suffer from external short-circuit. When such a fault occurs on the output line of the transformer, very high currents are pulled from the supply line of the transformer [1]. These very high currents generate heat and forces on windings that may be enormous. Standard measures to design transformers to withstand short circuit faults are provided in [2], where a standard duration of 2s is specified. During this time frame, winding temperature will increase due to the high current value. At the same time, high axial forces generated in the coil conductors are propagated across insulation elements, oil, clamping woods onto the core or tank [3]. For this reason, the tank is equipped with a specific structural short-circuit beam designed to withstand the impact of these high forces (case of a shell form transformer) [4].

The first design consideration is therefore the thermal effect brought on by the high short duration currents. As the thermal time constant of a winding is over 100 times greater than the maximum duration of the fault, it is acceptable to consider that all generated heat is retained in the conductors whose temperature will evidently rise. Analytical formulae or numerical methods may be employed to estimate the winding temperature rise, where [2] again provides maximum admissible temperatures for aluminum or copper conductors.

The second design consideration, on which this paper focuses upon, is the very high forces generated when the conductors are subject to the short circuit currents. Lying in a magnetic leakage field, conductors which carry current shall become loaded by a force of magnitude proportional to the square of that current [3]. The resultant force of a coil will be transmitted across paper and pressboard elements onto the adjacent coil. This situation repeats itself for all loaded coils. Because there are significant masses (mostly from the copper or aluminum conductors) and significant spring elements (pressboard, with non-linear characteristics), the problem of studying the movement of a winding must be performed in the dynamic domain. Clear description on the winding and core clamping schemes of shell form transformers can be found in [3][4].

In general, the structural parts of power transformers are made from non-alloy structural steel types but the selection process of the steel grade is sometimes based on the material stress response under quasi-static loading conditions derived from tensile tests performed in conventional universal testing machines (see for example [5]). Because the main goal of material selection for structural parts of power transformers is to improve mechanical performance, reduce weight and minimize costs while meeting the safety requirements during short-circuit faults, it follows that knowledge of the stress-strain mechanical behavior under medium to high rates of loading is crucial for choosing the steel grade and for designing shell form power transformers at the extreme conditions that are commonly found during short circuit faults.

The mechanical characterization of materials under different strain rate $\dot{\epsilon}$ loading conditions can be systematized into five categories; (i) mechanical characterization under extremely low rates of loading (say, $\dot{\epsilon} < 10^{-4} \text{ s}^{-1}$ and commonly designated as ‘the creep domain’), (ii) mechanical characterization under low rates of loading (say, $10^{-4} < \dot{\epsilon} < 10^{-1} \text{ s}^{-1}$ and designated as ‘the quasi-static domain’), (iii) mechanical characterization under medium rates of loading (say, $10^{-1} < \dot{\epsilon} < 10^2 \text{ s}^{-1}$ and designated as ‘the intermediate strain rate domain’), (iv) mechanical characterization under high rates of loading (say, $10^2 < \dot{\epsilon} < 10^5 \text{ s}^{-1}$ and designated as ‘the high strain rate domain’) and (v) mechanical characterization under very high rates of loading (say, $\dot{\epsilon} > 10^5 \text{ s}^{-1}$ and designated as ‘the ballistic or ultrahigh strain rate domain’) [6].

The importance of properly defining the strain rate loading conditions for designing shell form power transformers results from the generalized lack of information regarding the flow stress $\sigma(\epsilon, \dot{\epsilon})$ for strain rates acting above the quasi-static domain and may be considered one of the main reasons for designing structural elements to be more robust, heavier and more expensive than necessary for power transformers to fulfil the safety requirements.

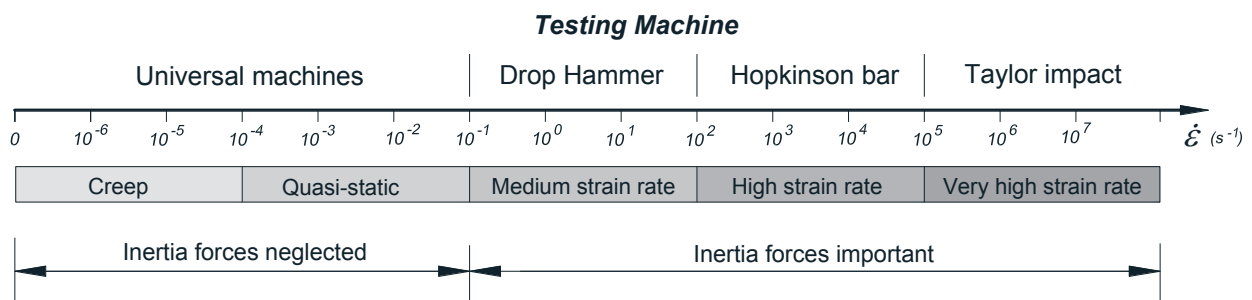


Figure 1. Strain rate operating conditions corresponding to different types of mechanical testing machines

Figure 1 presents an attempt to correlate the different types of mechanical testing machines used for material characterization with the operating conditions of strain rate that are required for a specific engineering application [3]. As seen, the mechanical characterization of materials in the creep and quasi-static strain rate domains is performed by the widely available universal testing machines operating under load, displacement or strain control. The mechanical characterization of materials in the intermediate strain rate domain is more difficult to perform and frequently involves the utilization of tailored designed drop weight (gravity), hydraulic or mechanical systems. Special purpose testing equipment based on slip Hopkinson pressure bars and Taylor impact systems are needed for the mechanical characterization of materials in the high and ultrahigh strain rate domains.

In case of material characterization for the structural parts of power transformers, the strain rate loading conditions need to be identical to those occurring in short circuit faults (around 100 s^{-1}) and , therefore, drop weight testing machines are the most adequate equipment.

This paper presents an in-house flexible drop weight testing machine to perform the mechanical characterization of the types of structural steel that are commonly used in the fabrication of shell form tanks. The flow stress $\sigma(\varepsilon, \dot{\varepsilon})$ derived from these tests is then used to obtain finite element estimates of the plastic deformation of the main structural components of a power transformer that was short circuit tested.

Results show that knowledge of the mechanical properties of the materials at medium to high strain rates is very important to estimate the plastic deformation of structural components that may arise from short circuits or other situations where the rate of loading is relatively high and the time period is short.

2. MECHANICAL CHARACTERIZATION

2.1. Equipment, methods and procedures

The investigation made use of three different types of non-alloy structural steel (S235JR, S275JR and S355JR) and a high strength structural steel (WELDOX 700). The mechanical characterization was performed by means of compression tests carried out on cylindrical test specimens with 6 mm diameter and 9 mm height that were manufactured from the supplied steel plates at strain rate levels of approximately 100 s^{-1} in order to match the loading rates originated in short circuit faults.

Figure 2 presents the in-house flexible drop weight testing machine where tests were performed with schematic charts showing its main operating features. For presentation purposes and although not corresponding to what readers directly observe in Figure 2a, the main components of the machine are split into three main groups: (1) structural, (2) mechanical and electrical, and (3) control and measurement.

The structural components of the machine comprise the frame and a plurality of individual parts that are independent of the material and mechanical tests to be performed such as, the pre-stressed columns, the anvil that holds the tool, and the support plates that are used for fixing the machine to the floor. The ram and its levering system, the tool and its active die accessories for each specific mechanical test to be performed are the most significant mechanical and electrical components. The equipment for monitoring the downward drop of the carriage and ram, the load cell, the displacement transducer, and the data acquisition system are the main control and measuring components.

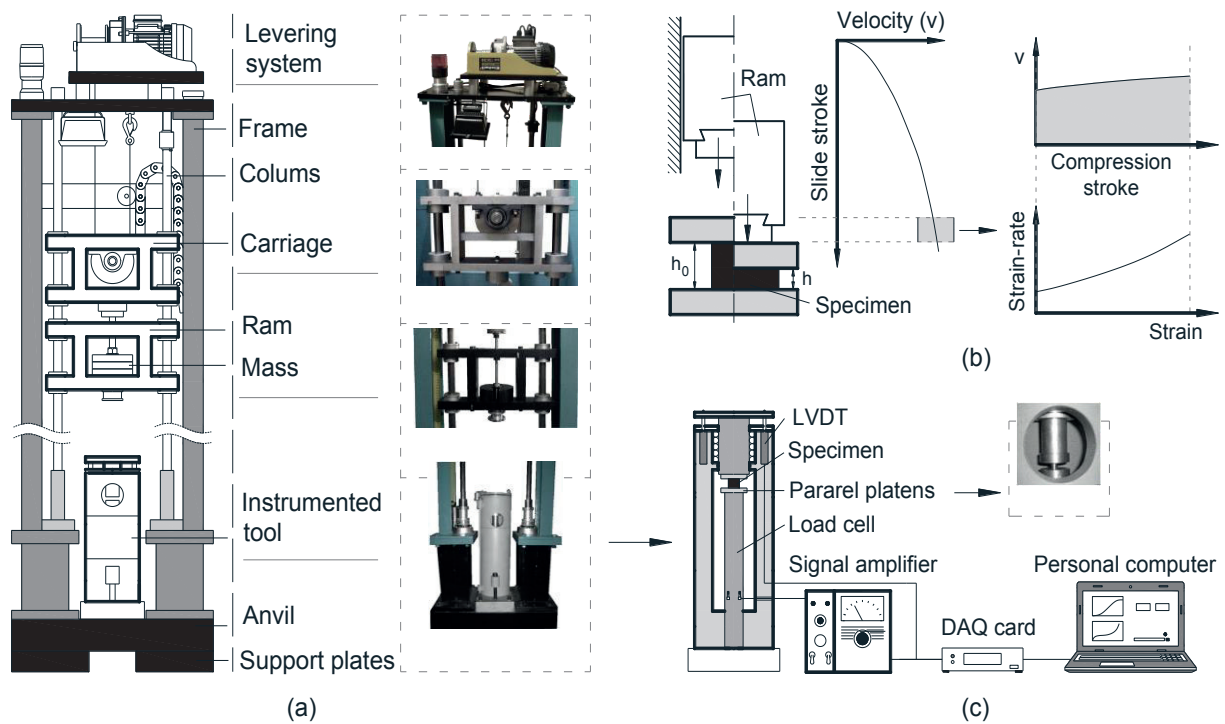


Figure 2: Flexible drop weight testing machine. (a) Schematic representation. (b) Velocity versus stroke and strain rate versus strain loading paths in the working region. (c) Detail of the tool equipped with a load cell and a displacement transducer.

The most important characteristic of this machine is the tailored-made operating conditions resulting from the flexible design of the ram and tool. In fact, the mass of the ram and the height of the fall can be easily changed so that velocity and energy of each test can be selected to match the desired strain rate loading conditions. The active die accessories of the tool can also be easily replaced in order to perform a wide variety of tests such as compression, friction, and fracture toughness, among others.

The load cell installed in the tool was fabricated by the authors and is based on traditional strain gage technology in full wheatstone bridge. The load cell has a capacity of 40 kN, a nominal sensitivity of 1 mV/V, and an accuracy class 0.7. The displacement transducer is a commercial linear variable differential transformer (LVDT Solartron AC15). Both the load cell and the displacement transducer are mounted inside the tool case where the active die components are installed (refer to the detail in Figure 2c). The load cell is connected to a signal amplifier unit (Vishay 2310B) and a personal computer data logging system based on a DAQ card (PCI-6115, National Instruments) combined with a special purpose LabView software acquires and stores the experimental data from both the load cell and the displacement transducer. The true stress and strain are determined from these experimental data as follows,

$$\sigma = \frac{F}{A} \quad \varepsilon = -\int_{h_0}^h \frac{dh}{h} = \ln \frac{h_0}{h} \quad (1)$$

where F is the experimentally measured force, A is the cross section of the compression test specimen and h and h_0 are the actual and initial height of the compression test specimens obtained from the displacement transducer.

The strain rate is determined as follows,

$$\dot{\varepsilon} = \frac{d\varepsilon}{dt} = \frac{1}{h} \frac{dh}{dt} \cong \frac{v}{h} \quad (2)$$

where v is the velocity of the testing machine.

2.2. High loading rate material test results

Figure 3 shows the stress-strain behavior of the four different types of steel obtained from compression tests before and after filtering the oscillations that are commonly found at the beginning of these curves as a result of the dynamic loading testing conditions. The fitted curves after filtering the oscillations are drawn in black and the results of compression tests performed in a universal mechanical testing machine under quasi static loading conditions are included in red for comparison purposes.

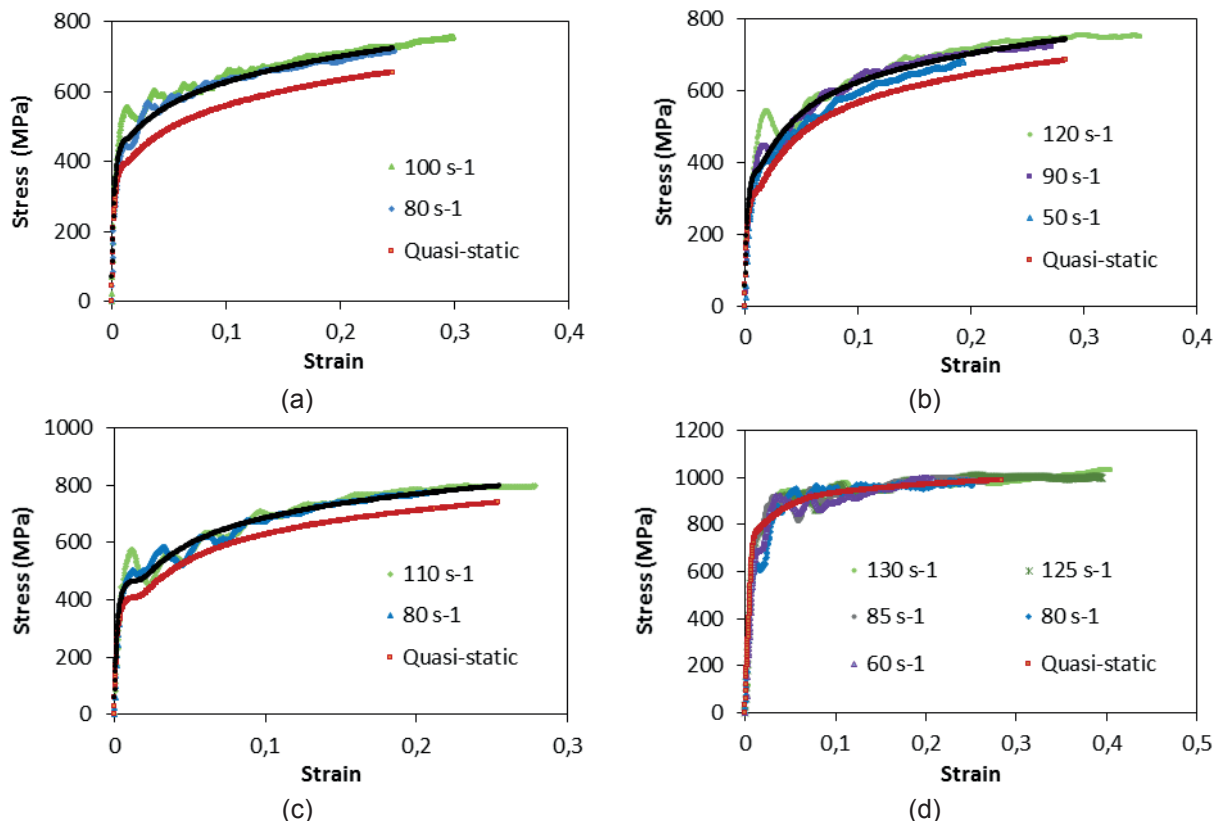


Figure 3: True stress-strain curves of the (a) S235JR, (b) S275JR, (c) S355JR and (d) WELDOX 700 types of structural steel obtained from compression tests at different strain rates

As seen in Figures 3a, 3b and 3c, the stress response of non-alloy structural steel S235JR, S275JR and S355JR increases by approximately 60 MPa~70 MPa when the strain rate loading conditions are increased from quasi-static to 100 s⁻¹. In contrast, Figure 3d, allows concluding that the stress response of the high strength structural steel WELDOX 700 remains practically unchanged when the strain rate loading conditions are increased from quasi-static to values at the vicinity of 100 s⁻¹.

3. APPLICATION OF TEST RESULTS TO SHORT-CIRCUIT DESIGN

GROPTI™ is a software tool that has been developed to estimate displacements, velocities and accelerations of winding and tank structural elements [3]. It is an EFACEC proprietary tool developed specifically to analyze shell form transformer motions during short circuit events. Through the incorporation of a carefully built genetic algorithm, the tool not only allows for the precise estimation of the movement of coils but also provides optimal design of the tank's short-circuit beams.

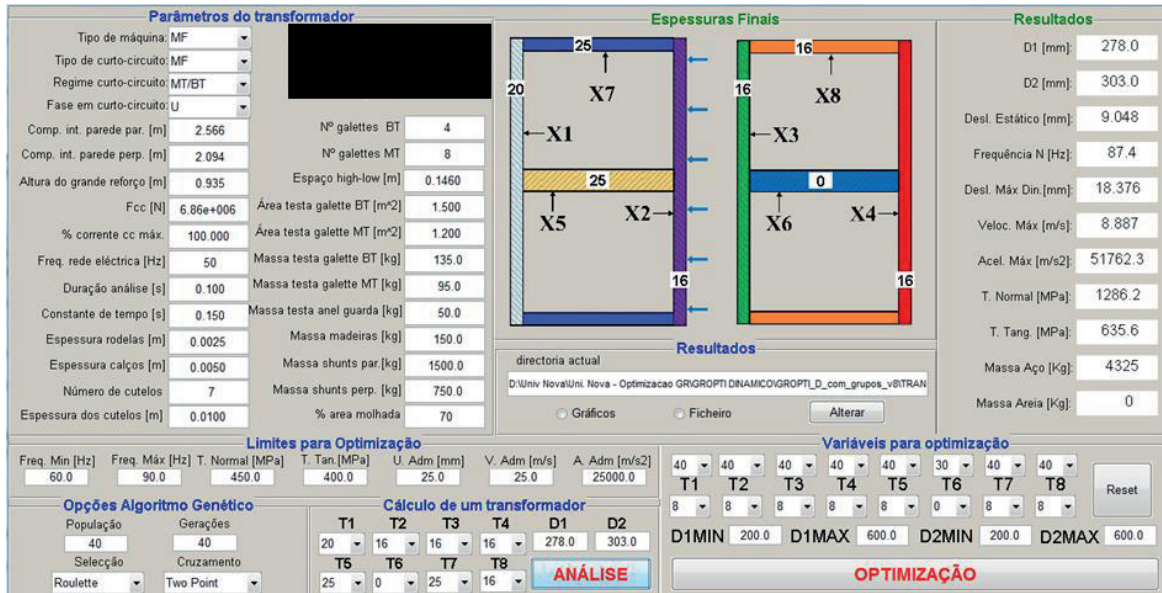


Figure 4: The GROPTI GUI. The software can evaluate the short circuit response of the coil groups, or it may determine the plate thicknesses for the box beam elements such that system response is according to specified user requirements

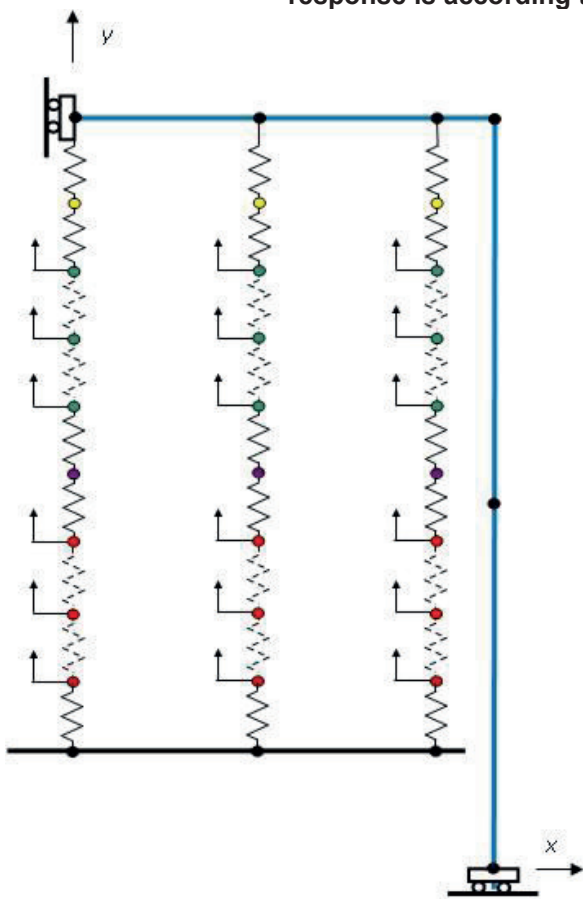


Figure 5 The FEM model that is automatically created with GROPTI for analyzing system response. The number of masses (representing coils) and springs (pressboard) vary with each short circuit, as does the application of coil forces on masses.

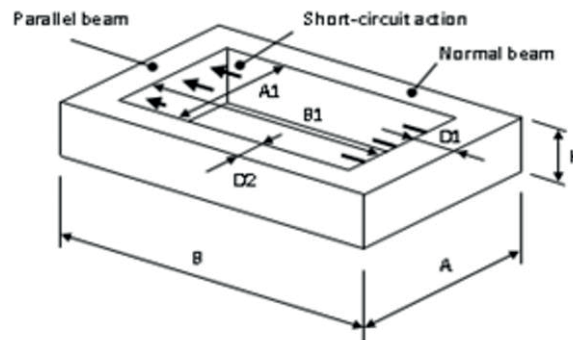


Figure 6: Some GROPTI parameters ('normal beam' also referred as 'perpendicular beam')

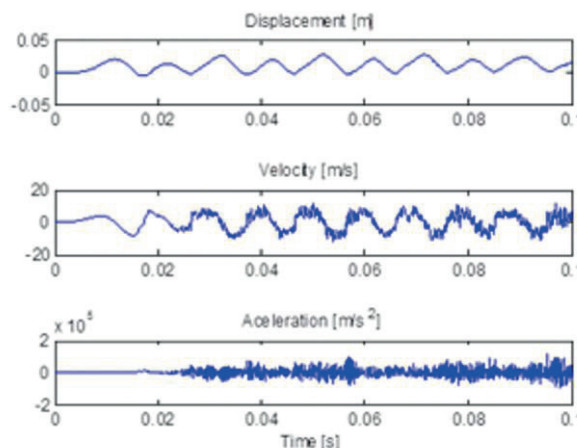


Figure 7: Displacement, velocity and acceleration of box beam mid-span during a short circuit. These outputs are graphical; other outputs are also given on the GROPTI GUI, such as material stress or box beam natural frequency

3.1. APPLICATION EXAMPLE: Transformer description and force evaluation

This example is taken from a transformer that was short circuit tested. It is a 50Hz 100MVA 400kV ONAN/ONAF/ODAF single phase autotransformer with a tertiary winding. Figure 8 shows the series winding in red, the common in green and the tertiary in blue.

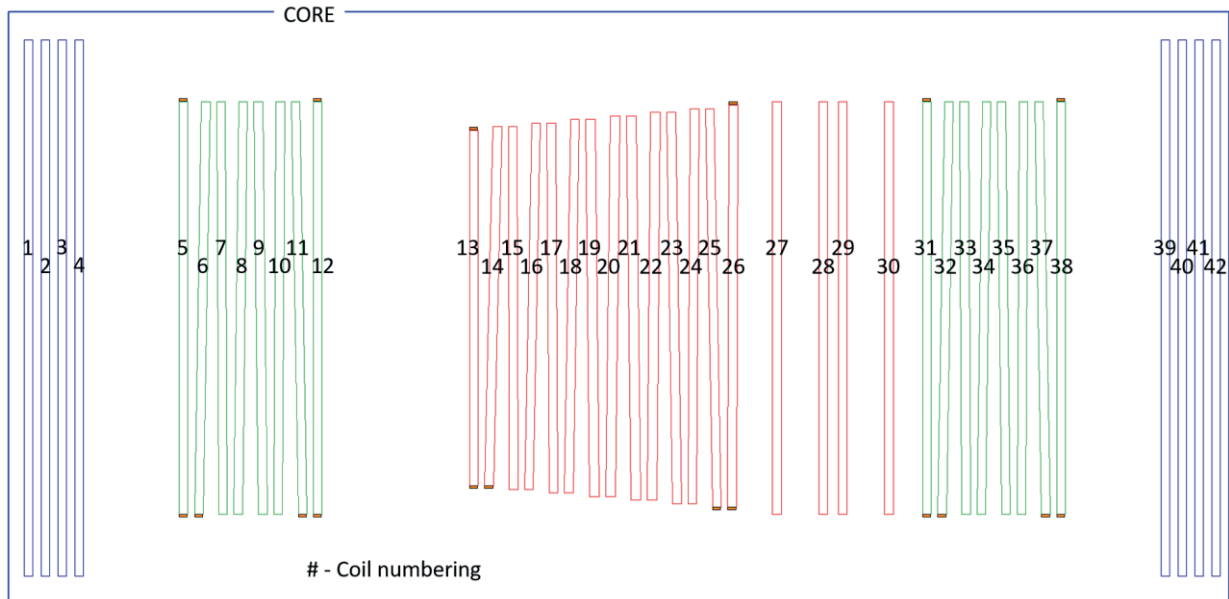


Figure 8: Window cutaway and coil numeration of transformer being short circuit tested

The first step of the process is the definition of the short circuit scenario that is going to be tested. Once the worst case short circuit was identified, a model of the transformer was built (see Figure 9) and the appropriate short circuit currents were introduced (these currents were defined based on the methodology in [2]).

Figure 10 shows the introduction of the currents into the model, where the different colors indicate currents in phase opposition. In this case, it is the common winding and the series winding that are in a short-circuit condition, whereas the tertiary winding is kept open circuited. A graph of the accumulated ampere-turns of the transformer during the fault is shown in Figure 11.

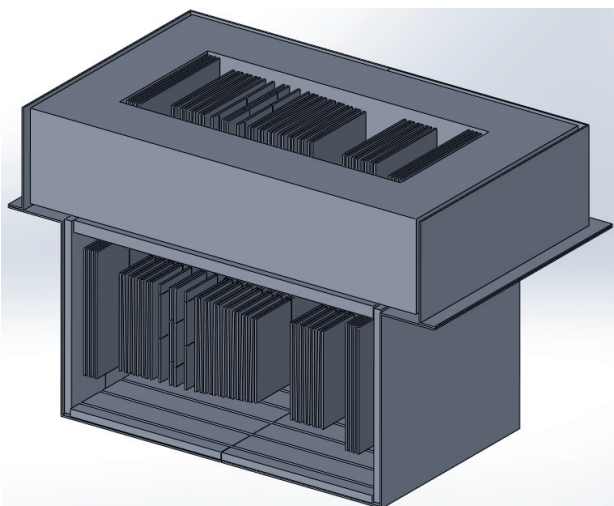


Figure 9: 1/4 transformer model for short circuit coil axial force evaluation with two symmetry planes



Figure 10: Short circuit condition being tested. Different colors represent opposing currents

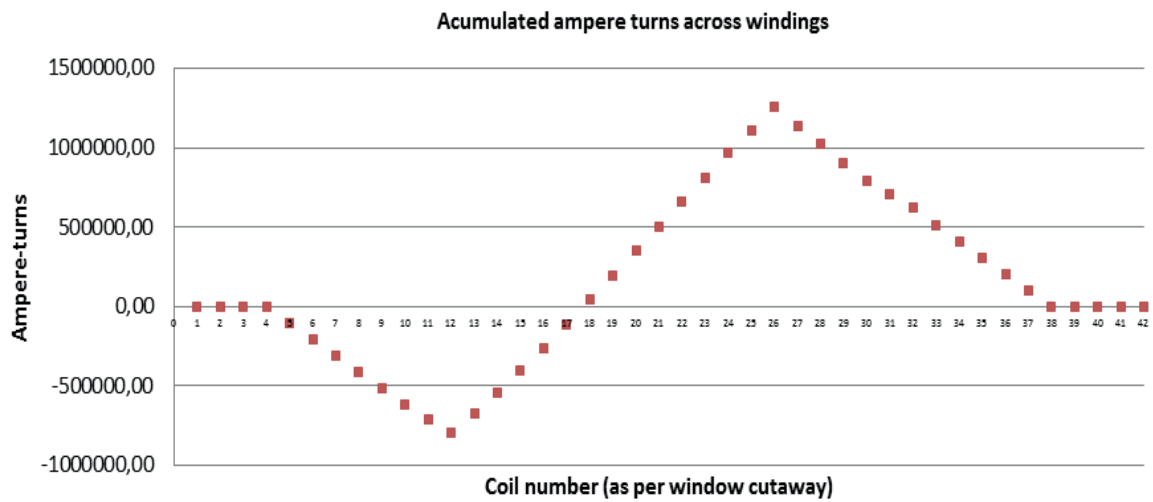


Figure 11: Graph of accumulated ampere-turns for each coil across windings

The numerical analysis of the described model yields magnetic field distributions. A boundary element method (BEM) program was used for a magnetostatic operation mode analysis. The resulting leakage induction field plot at the window cutaway symmetry plane are shown in Figure 12 and in Figure 13. Forces will be generated at coils due to this leakage and due to the current going through the conductors. Peak values for these forces are shown in Figure 14, where both the axial force acting on each coil together with the force accumulation across the window are shown. Figure 15 then shows a subdivision of the forces acting on the areas directly opposing the magnetic circuit from the forces acting on the areas directly opposing the short circuit beams. This is a very important separation to make, as the magnetic circuit shall withstand the former forces and the short circuit beams shall withstand the latter ones.

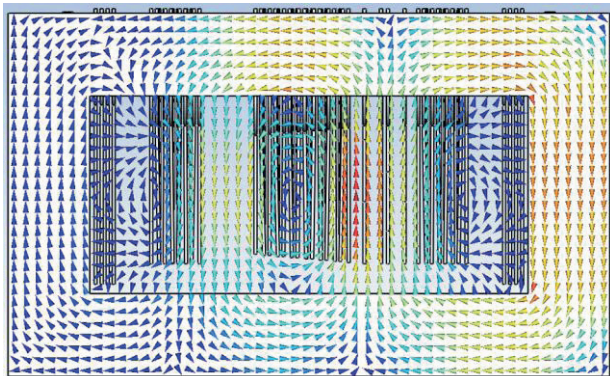


Figure 12: Leakage B-field arrow distribution at window section

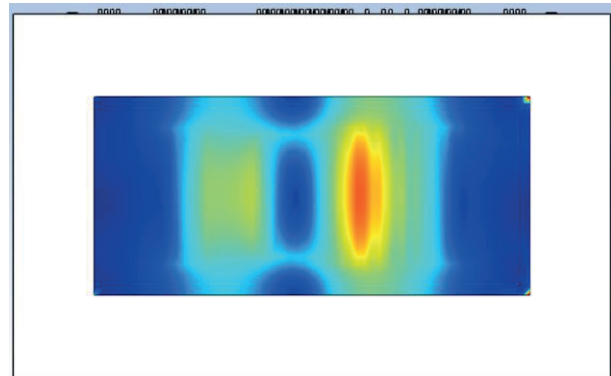


Figure 13: B-field intensity plot

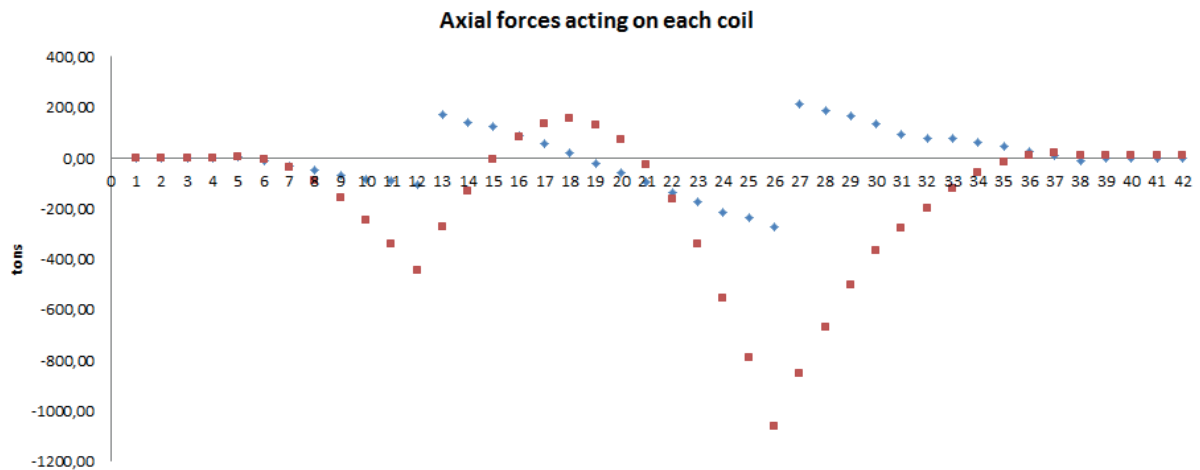


Figure 14: The blue (diamond shape graph) is the electromagnetic axial force acting on each coil, and in red is the correspondent accumulated axial force

From Figure 15 we can estimate that the peak total accumulated force acting on each short circuit beam is approximately 250 tons (this number can be found by summing all blue diamonds of Figure 15).

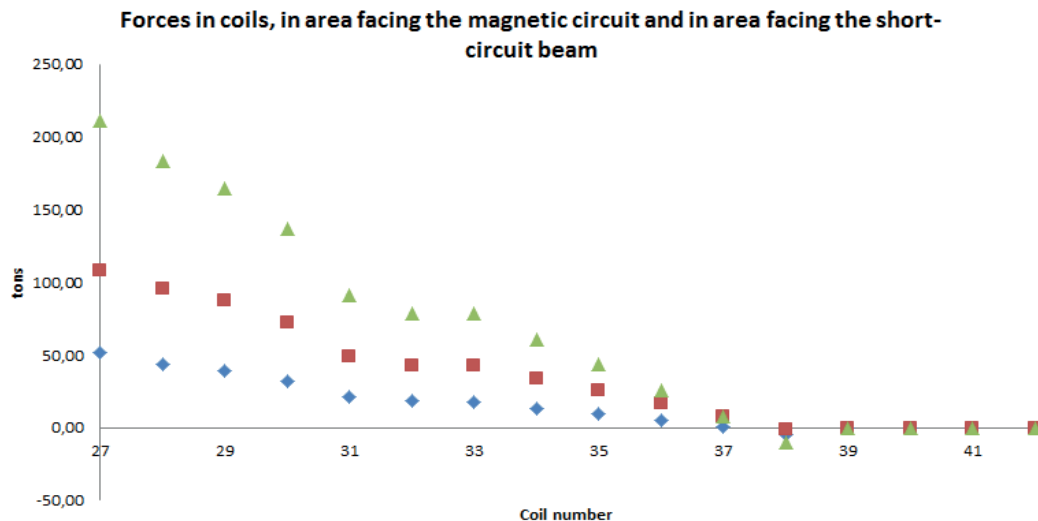


Figure 15: Axial forces in coils 27 through 42 (green triangles), with the forces acting on the areas facing the magnetic circuit (red squares) separated from the forces acting directly on the area facing the short circuit beam (blue diamonds). Note that there is always a lower and an upper short circuit beam.

3.2. GROPTI estimates for tank and coil movements

Once force estimates have been found, these may be introduced into the GROPTI software. Together with the forces, it is necessary to introduce several other input data parameters, such as the type of short circuit being analyzed, single/three phase geometry analysis, frequency, duration, line and transformer time constant, transformer geometrical dimensions, pressboard thicknesses, number of high and low voltage coils, mass of coils, impact area, mass of compression woods and static shields, magnetic shunt masses and wet area (area of oil in contact with insulated conductors). Thicknesses of steel plates used to build the short circuit beam are also necessary. These inputs are all inserted into the GUI shown in Figure 4.

Following its analysis, GROPTI outputs results, both in the GUI and in graphical format (see Figure 16). The main results are: coil and beam natural frequencies, maximum beam center point displacement, maximum beam velocity, beam peak acceleration, maximum normal stress in beam, maximum tangential stress and also the estimated beam mass.

GROPTI is also able to determine a good solution for the short circuit beam through its built in genetic algorithm. This optimization analysis requires that further inputs are given, such as for example genetic algorithm parameters, optimization constraints or acceptable range for optimization variables.

GROPTI assumes that the short circuit beam's steel is loaded in its elastic domain. In reality, there is always some plasticity that leads to permanent plastic deformation. It is important to understand the level of permanent plastic deformation which is left, as this will impact transformer properties.

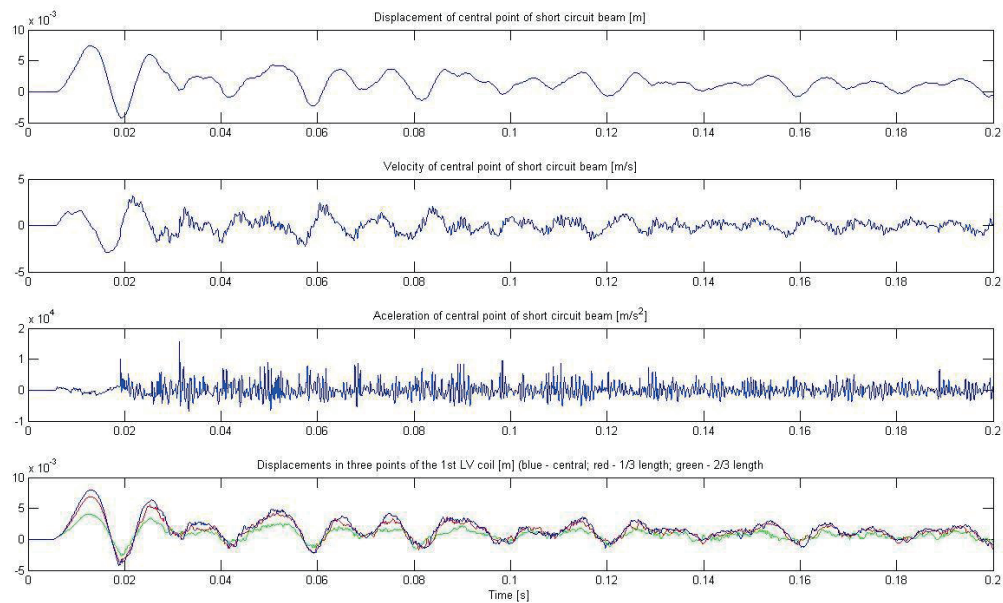


Figure 16: GROPTI displacement, velocity and acceleration results for the short circuit beam and selected coils, for the transformer that is being analyzed

4. ESTIMATION OF PERMANENT BEAM DEFORMATION

At this point we have in hand the motion estimates which assume material linearity, and we wish to assess the level of plastic deformation of the beam. In particular we are interested in determining the permanent configuration of the beam, that is, the configuration of the beam once all loads are removed. Permanent plastic deformation may be found by applying an equivalent energy method. There are 2 steps involved:

1. Assuming material linearity, determine the equivalent static force that causes the maximum dynamic displacement given by GROPTI, and compute the elastic deformation energy absorbed by the beam in that condition;
2. Apply the nonlinear material to the beam, and apply a force such that the total (elastic + plastic) deformation energy equals the elastic deformation energy of step 1.

Due to plasticity being present, even if in small proportions, it is always the case that for an equivalent energy there will always be more displacement with the nonlinear material. Residual deformation is unwanted as it will alter transformer properties permanently; therefore only very small residuals are tolerated.

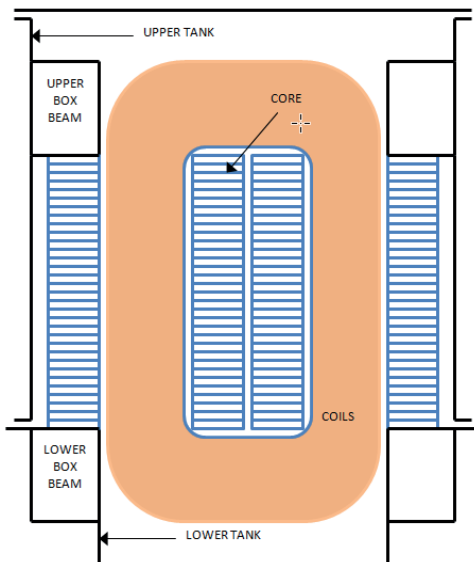


Figure 17: Location of short circuit beam in transformer tank

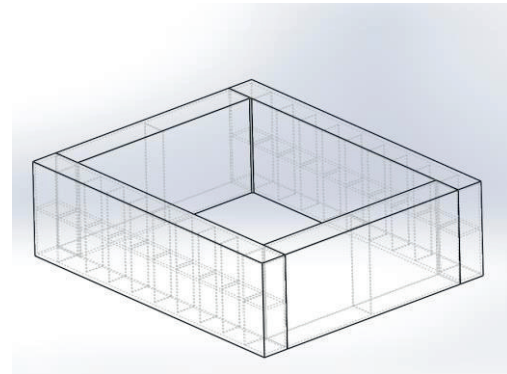


Figure 18: Short circuit box beam shown isolated from transformer. Can be seen as the upper or lower box beam of Figure 17

The procedure that has been outlined to estimate the permanent plastic deformation will be applied in two different situations. First, we shall consider that the dimensions of the beam are fixed, and we shall vary the steel material applied to the beam and then check for the residuals. Secondly, we shall design the beam for each one of the four steel materials under consideration (using GROPTI), attempting to have the same residuals for each case, so that solutions may be compared to each other.

4.1. Fixed beam solution

By applying the described procedure to the beam dimensions (that were effectively fabricated), we obtain the results of Table 1.

Table 1: FEM simulation results applying the four different types of steel (same beam for all)

FIXED BEAM SOLUTION		S235JR	S275JR	S355JR	WELDOX700
Beam mass	kg	4325	4325	4325	4325
Total deformation energy	MJ	10	10	10	10
Max Von Mises stress at corner	MPa	337	406	402	990
Max Von Mises stress at midspan	MPa	218	238	194	237
Max displacement at midspan	mm	7.46	7.46	7.49	7.45
Max residuals at midspan	mm	0.07	0.02	0.21	0

For all types of steel considered, residuals may be considered “zero”, behavior is still very linear. Even though stress levels at corners are well beyond the elastic limits, plasticity domains at the corners have little effect on the residual values. As the material curves used for the simulation were taken from the experimental results, slight deviations may occur that can well explain the slightly higher residual value for the S355JR steel. Figure 19 and Figure 20 show displacement results for the S355JR steel (the FEM package used was ANSYS 11.0, with mechanical static structural and material nonlinear simulations).

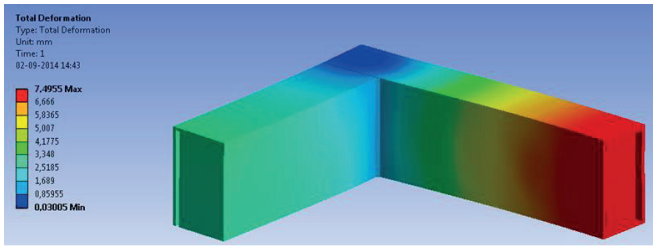


Figure 19: Beam maximum displacements (1/8 model used) for the S355JR steel

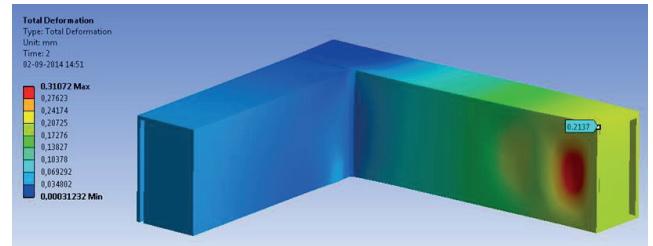


Figure 20: Maximum residual displacements (or permanent beam configuration) following load removal on the S355JR steel beam

4.2. Variable beam solution

The procedure described in the beginning of this section was then applied to 4 different beam solutions, each solution matching one of the types of steel. The beam solutions were generated by the optimization algorithm contained in GROPTI. Moreover, the solutions were sought taking in consideration the particular constraints that existed in this transformer. Should the constraints change then the solutions that are achieved as 'optimal' may change too. Table 2 shows the results for each one of the 4 solutions.

Table 2: FEM simulation results for optimal beams for all four types of steel (all beams different)

VARIABLE BEAM SOLUTION		S235JR	S275JR	S355JR	WELDOX700
Beam mass	kg	4000	3900	3580	2610
Mass variation wrt S235JR	%	-	-2.5%	-10.5%	-35%
Total deformation energy	MJ	10	10	12	14
Max Von Mises stress at corner	MPa	322	412	420	1008
Max Von Mises stress at midspan	MPa	218	278	226	403
Max displacement at midspan	mm	7.52	7.91	9.52	13.9
Max residuals at midspan	mm	0.05	0.05	0.66	0

Two points are worth mentioning. Firstly, these results confirm the 'common sense' assumption that better steel grades lead to lighter weight solutions. The answer to the question of which steel is most cost wise efficient will depend greatly on the unit acquisition price of the steel together with fabrication costs and other possible cost issues such as for example transportation costs. Nevertheless, the results from Table 2 provide a guideline to how the mass of a short circuit beam may change with application of different types of steel. Secondly, the solution shown for the WELDOX700 steel has nearly twice the admissible displacement when compared to the S235JR steel. It has become clear that higher displacements accompany higher grade steel types, up to a point where the transformer engineer does not allow for higher displacements above a certain limit. The lower grade steel would not be capable of producing the same higher displacements without increasing its stress levels and therefore compromising its permanent plastic deformation values.

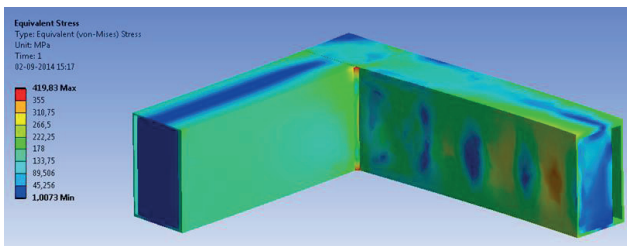


Figure 21: Stress fields in the S355JR steel

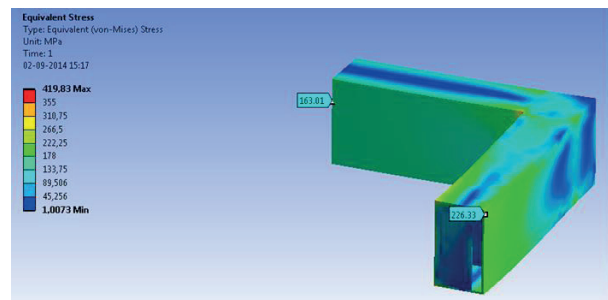


Figure 22: Stress fields from a different angle

As a last note, transformer impedance varies following a short circuit. There are movements in the coils and the phase settles to a (slightly) different configuration once forces cease. Many factors influence the impedance variation, and the good performance of the short circuit beam is only one of

them. Assurance that beam configuration settles back to its original configuration, less any residuals that may be neglected, is a necessary but not sufficient condition for impedance variation values to be within tolerances. But it is certainly one that is within the transformer manufacturer's control to assure.

5. CONCLUSIONS

Loading speed increases the energy absorbing capability of structural steel. This was found true for the lower grade (more common) steel and not true for the high grade (higher end) steel. At speeds close to 100Hz, differences in between common and high grade steel diminish, due to the enhanced performance of common steel at higher speeds. Another fact that is sometimes overlooked is that to take full advantage of a higher yield and tensile stress, higher grade steel solutions must allow for larger displacements, which are not desirable from a short circuit control standpoint. If larger displacements are not allowed, then differences in between common and higher grade types of steel are further diminished, as the higher grade structural steel is underutilized.

REFERENCES

- [1] K. Karsai, D. Kerényi, L. Kiss, "Large Power Transformers", Elsevier, 1987.
- [2] IEC 60076-5 : 2006, "Power Transformers – Part 5 : Ability to withstand short-circuit"
- [3] E. Almeida, P. Pedro, J. Cardoso, R. Ribeiro, "Design and dynamic analysis of shell form transformers under short-circuit conditions", Cigré Colloquium, Zurich, Switzerland, 2013.
- [4] J. Thierry, "Core-form and shell form transformers: Applications, design and construction", Life of a Transformer Seminar, Lake Buena Vista, Florida, USA, 2014.
- [5] E. Almeida, H. Mendes and A. Pinho, "Experimental validation of a CORE type power transformer tank", in Proceedings ASME International Mechanical Engineering Congress and Exposition, November, 2009.
- [6] C.M.A Silva, P.A.R. Rosa, P.A.F. Martins, "Innovative Testing Machines and Methodologies for the Mechanical Characterization of Materials", Experimental Techniques, 2014 (in press doi:10.1111/ext.12094).